Simulation of Switched Reluctance Motor Drives Using Two-Dimensional Bicubic Spline

Xiang-Dang Xue, K. W. E. Cheng, *Member, IEEE*, and S. L. Ho

***Abstract*—In this paper, a novel simulation algorithm of switched reluctance motor drives is presented. With the proposed algorithm the two-dimensional (2-D) bicubic spline interpolation is used to describe the nonlinear magnetic characteristics in switched reluctance motors. The corresponding computational method of 2-D bicubic spline function is described in detail. The simulation results are also compared with and validated by experimental data. Compared with conventional techniques, the presented simulation algorithm is more accurate even though it requires relatively little information on the magnetic characteristics of the motor.**

***Index Terms*—Bicubic spline, simulation, switched reluctance motor drives.**

I. Introduction

SWITCHED reluctance motors are well-known to be highly saturated magnetically due to their intrinsic physical characteristics, therefore models of switched reluctance motors are based generally on nonlinear first order derivative equations. The characteristics of flux linkage with respect to both rotor position angle and current are generally required before one attempts to solve the nonlinear first order derivative equation. In order to realize computer-aided design, performance prediction, simulation study and real time control accurately and speedily, many researchers have been modeling the characteristics of flux linkage with respect to rotor position angle and current for many years. The previous studies [1]–[11] to model the nonlinear magnetic characteristics in switched reluctance motors can be summarized as follows.

1) One-dimensional (1-D) piecewise linear function [4], [11].
2) One-dimensional piecewise quadratic function [3].
3) One-dimensional analytic function [5], [7].
4) Two-dimensional (2-D) piecewise analytic function [6], [8], [9].
5) Sinusoidal function [10].
6) One-dimensional cubic spline function [1], [2].

However, an ideal interpolation function to model the real magnetic characteristics in switched reluctance motors should not simply be expressed as a discrete function of both rotor position angles and phase currents. It should give accurate interpolated values as well. The interpolation functions as reported [1]–[11] does not have these two features simultaneously.

In this paper, the 2-D bicubic spline function is regarded as the interpolation function to model experimental data of the magnetic characteristics in switched reluctance motors. The interpolation of the flux linkage with respect to rotor position angle and current based on this function is quite accurate, as 2-D bicubic spline function is a third-order function [12]. It can be seen that the interpolation function presented in the paper is different from the previous methods and is more accurate than the previous ones [3]–[11]. Moreover, as flux linkage is directly dependent on both rotor position angle and current, an interpolation function describing the magnetic characteristics in switched reluctance motors is expected to yield more accurate results swiftly [1], [2]. The authors will describe in detail the computational procedures for finding the coefficients of the 2-D bicubic spline function. The simulation and experimental results show that the presented simulation algorithm is highly accurate and robust.

II. Two-Dimensional Bicubic Spline Interpolation

A. Two-Dimensional Bicubic Spline Function

Flux linkage is a function of both rotor position angle and phase current. Hence, flux linkage Ψ can be expressed as the third dimensional quantity sitting on a 2-D plane comprising the rotor position angle θ and phase current i. Moreover, these two variables can vary within the limited regions according to the symmetry and periodicity in the switched reluctance motors. In general, one has $\theta_{on} \le \theta \le (\theta_{on}+\theta_T)$ and $0 \le i \le i_{\max}$ where θ_{on} represents the turn-on angle, θ_T represents the inductance period of switched reluctance motor and $i_{\max}$ represents the maximum phase current. Therefore, this is a rectangular region.

Suppose that small amount of *a prior* discrete data about flux linkage with respect to rotor position angle and current are obtained through FEM or experiment, one has $\theta_{on} = \theta_1 < \theta_2 < \cdots < \theta_{k-1} < \theta_k < \theta_{k+1} < \cdots < \theta_N = (\theta_{on} + \theta_T)$ and $0 = i_1 < i_2 < \cdots i_{j-1} < i_j < i_{j+1} < \cdots < i_M = i_{\max}$ where $N \ge 2$, $M \ge 2$, N represents the number of rotor position angles and M represents the number of currents data.

The above rectangular region is firstly subdivided into $(N-1)(M-1)$ subrectangles. Arbitrarily, one of these rectangles is assumed to be a subrectangle R_{kj} with vertices, (θ_k, i_j), (θ_{k+1}, i_j), (θ_{k+1}, i_{j+1}) and (θ_k, i_{j+1}), where $1 \le k \le (N-1)$

Manuscript received May 2, 2001; revised February 1, 2002. This work was supported by the RGC of Hong Kong under Project PolyU5085/98E, and the Research Committee,Hong Kong Polytechnic University under Project G-W081.

X.-D. Xue is with the Department of Electrical Engineering, Hong Kong Polytechnic University, Hung Hom, Kowloon, Hong Kong (e-mail: xdxue.ee@polyu.edu.hk).

K. W. E. Cheng and S. L. Ho are with the Department of Electrical Engineering, Hong Kong Polytechnic University, Hong Kong (e-mail: eeecheng@polyu.edu.hk; eeslho@polyu.edu.hk).

Digital Object Identifier 10.1109/TEC.2002.805226

and $1 \le j \le (M-1)$, then the proposed 2-D bicubic spline function on a subrectangle R_{kj} can be written as follows:

$$\Psi(\theta,i) = (g_{k1}(\theta), g_{k2}(\theta), g_{k3}(\theta), g_{k4}(\theta))\, A \begin{pmatrix} g_{j1}(i) \\ g_{j2}(i) \\ g_{j3}(i) \\ g_{j4}(i) \end{pmatrix} \quad (1)$$

where $\theta_k \le \theta \le \theta_{k+1}$, $i_j \le i \le i_{j+1}$, the g_{kl} and g_{jl} satisfy ($l = 1, 2, 3, 4$)

$$\begin{cases} g_{k1} = 1 \\ g_{k2} = \theta - \theta_k \\ g_{k3} = (\theta-\theta_k)^2 \\ g_{k4} = (\theta-\theta_k)^3 \end{cases}, \begin{cases} g_{j1} = 1 \\ g_{j2} = i - i_j \\ g_{j3} = (i-i_j)^2 \\ g_{j4} = (i-i_j)^3 \end{cases} \quad (2)$$

and the matrix A is 4×4

$$A = \begin{pmatrix} a_{kj11} & a_{kj12} & a_{kj13} & a_{kj14} \\ a_{kj21} & a_{kj22} & a_{kj23} & a_{kj24} \\ a_{kj31} & a_{kj32} & a_{kj33} & a_{kj34} \\ a_{kj41} & a_{kj42} & a_{kj43} & a_{kj44} \end{pmatrix}. \quad (3)$$

Any flux linkage value can be computed from (1) if the coefficients in the matrix A are known. For each subrectangle R_{kj}, there are 16 coefficients in (3). However, there are $16(N-1)(M-1)$ coefficients for whole rectangular region R. The total of $16(N-1)(M-1)$ coefficients must be defined.

B. Definition of Matrix A and Computation of the Coefficients

For each subrectangle R_{kj}, the bicubic spline interpolation requirements give four conditions, which are function values $\Psi(\theta_k, i_j)$ of four nodes of the subrectangle. Therefore, one still needs to introduce a total of 12 temporary unknowns or parameters in order to define matrix A. Here, the choice for these is that of the values of the first partials and the mixed partials derivative at each of the four nodes of the subrectangle.

In this case, the matrix A is to be determined form the following matrix C:

$$C = \begin{pmatrix} \Psi_{kj} & q_{kj} & \Psi_{k,j+1} & q_{k,j+1} \\ p_{kj} & r_{kj} & p_{k,j+1} & r_{k,j+1} \\ \Psi_{k+1,j} & q_{k+1,j} & \Psi_{k+1,j+1} & q_{k+1,j+1} \\ p_{k+1,j} & r_{k+1,j} & p_{k+1,j+1} & r_{k+1,j+1} \end{pmatrix}. \quad (4)$$

If one write the partial derivatives of (1), then the connection matrix V can be obtained

$$V(\theta_k) = \begin{pmatrix} g_{k1}(\theta_k) & g_{k2}(\theta_k) & g_{k3}(\theta_k) & g_{k4}(\theta_k) \\ g'_{k1}(\theta_k) & g'_{k2}(\theta_k) & g'_{k3}(\theta_k) & g'_{k4}(\theta_k) \\ g_{k1}(\theta_{k+1}) & g_{k2}(\theta_{k+1}) & g_{k3}(\theta_{k+1}) & g_{k4}(\theta_{k+1}) \\ g'_{k1}(\theta_{k+1}) & g'_{k2}(\theta_{k+1}) & g'_{k3}(\theta_{k+1}) & g'_{k4}(\theta_{k+1}) \end{pmatrix} = \begin{pmatrix} 1 & 0 & 0 & 0 \\ 0 & 1 & 0 & 0 \\ 1 & \Delta\theta_k & \Delta\theta_k^2 & \Delta\theta_k^3 \\ 0 & 1 & 2\Delta\theta_k & 3\Delta\theta_k^2 \end{pmatrix}. \quad (5)$$

Therefore, (1) and (4) satisfy the following relation:

$$C = V(\theta_k)\, A\, [V(i_j)]^t \quad (6)$$

where $[V(i_j)]^t$ is the transfer matrix of $V(i_j)$.

Solving (6), (7) can be obtained

$$A = [V(\theta_k)]^{-1}\, C\, [V(i_j)]^{-t}. \quad (7)$$

The function values of four nodes in C are known. The other coefficients in C can be computed from (8)–(11).

For $j = 1, \ldots, M$, one has

$$\frac{1}{\Delta\theta_{k-1}} p_{k-1,j} + 2\left[\frac{1}{\Delta\theta_{k-1}} + \frac{1}{\Delta\theta_k}\right] p_{kj} + \frac{1}{\Delta\theta_k} p_{k+1,j} = 3\left[\frac{\Psi_{kj} - \Psi_{k-1,j}}{\Delta\theta_{k-1}^2} + \frac{\Psi_{k+1,j} - \Psi_{kj}}{\Delta\theta_k^2}\right], \quad k = 2, \ldots, N-1. \quad (8)$$

For $k = 1, \ldots, N$, (9) exists

$$\frac{1}{\Delta i_{j-1}} q_{k,j-1} + 2\left[\frac{1}{\Delta i_{j-1}} + \frac{1}{\Delta i_j}\right] q_{kj} + \frac{1}{\Delta i_j} q_{k,j+1} = 3\left[\frac{\Psi_{kj} - \Psi_{k,j-1}}{\Delta i_{j-1}^2} + \frac{\Psi_{k,j+1} - \Psi_{kj}}{\Delta i_j^2}\right], \quad j = 2, \ldots, M-1. \quad (9)$$

For $j = 1$ and $j = M$, (10) can be obtained

$$\frac{1}{\Delta\theta_{k-1}} r_{k-1,j} + 2\left[\frac{1}{\Delta\theta_{k-1}} + \frac{1}{\Delta\theta_k}\right] r_{kj} + \frac{1}{\Delta\theta_k} r_{k+1,j} = 3\left[\frac{q_{kj} - q_{k-1,j}}{\Delta\theta_{k-1}^2} + \frac{q_{k+1,j} - q_{kj}}{\Delta\theta_k^2}\right], \quad k = 2, \ldots, N-1. \quad (10)$$

For $k = 1, \ldots, N$, we have

$$\frac{1}{\Delta i_{j-1}} r_{k,j-1} + 2\left[\frac{1}{\Delta i_{j-1}} + \frac{1}{\Delta i_j}\right] r_{kj} + \frac{1}{\Delta i_j} r_{k,j+1} = 3\left[\frac{p_{kj} - p_{k,j-1}}{\Delta i_{j-1}^2} + \frac{p_{k,j+1} - p_{kj}}{\Delta i_j^2}\right], \quad j = 2, \ldots, M-1 \quad (11)$$

where $\Delta\theta_k = \theta_{k+1} - \theta_k$ and $\Delta i_j = i_{j+1} - i_j$.

The total coefficients of the spline interpolation functions can be computed iteratively through equations from (4)–(11). The flow chart of computing the interpolation coefficients in bicubic spline function is shown in Fig. 1. A more detailed description is seen in [12].

III. Simulation

Fig. 2 shows the schematic diagram of switched reluctance motor drives. It illustrates a typical construction of switched reluctance drives. u_a, u_b and u_c represent the three-phase sinusoidal voltages. i_a, i_b and i_c represent three-phase ac currents. i is the dc current of the rectifier output. i_{cap} is the current of the capacitor. u_{cap} represents the voltage across the capacitor. i_{dc} is the dc input current of the topology circuit. C_p represents the capacitor.

Referring to Fig. 2, the modeling of switched reluctance motor drives with voltage source should satisfy the following equations, at steady state

$$i = i_{cap} + i_{dc} \quad (12)$$

$$i_{dc} = \sum k_p i_{wp} \quad (13)$$

$$\frac{d\Psi}{d\theta} = \frac{1}{\omega_r}(u_w - r_a i_w) \quad (14)$$

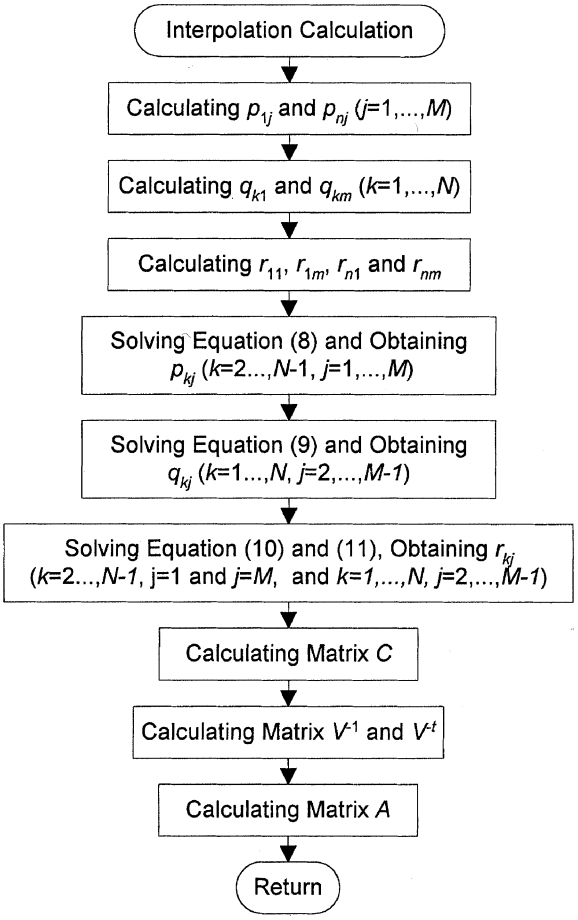

Fig. 1. Flow chart of computation of the interpolation coefficients in bicubic spline function.

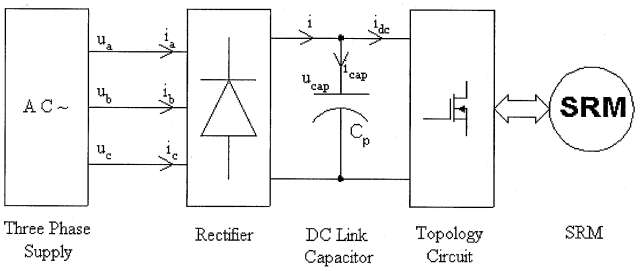

Fig. 2. Schematic diagram of switched reluctance motor drives.

$$u_w = \begin{cases} u_{dc} - 2^* v_T & when: s_t = 1 \\ -(u_{dc} + 2^* v_D) & when: s_t = -1 \\ -(v_T + v_D) & when: s_t = 0 \end{cases} \tag{15}$$

$$i_{cap} = C_p \frac{du_{cap}}{dt} \tag{16}$$

$$u_{cap}(t) = u_{cap}(t_0) + \frac{1}{C_p}\int_{t_0}^{t} i_{cap}(t)dt \tag{17}$$

$$u_{cap}(t) = u_{mn}(t) - v_R \; when: (u_{mn}(t) - v_R) > u_{cap}(t) \tag{18}$$

$$\theta = \omega_r t \tag{19}$$

where k_p is a coefficient that depends on the structure of the circuit topology, control strategy and switching angles and could be equal to 1, -1 or zero, i_{wp} represents phase currents in SRM, Ψ represents flux linkage of phase winding, θ represents the rotor position angle, ω_r represents the angular velocity of rotor, s_t is a coefficient, depending on the status of a winding, would be equal to 1, -1 or zero, u_w represents the winding voltage which is dependent upon s_t, i_w represents the current of the computed phase in the simulation, v_T is the on-state voltage of the IGBT, v_D is the forward voltage drop of the recovery diode

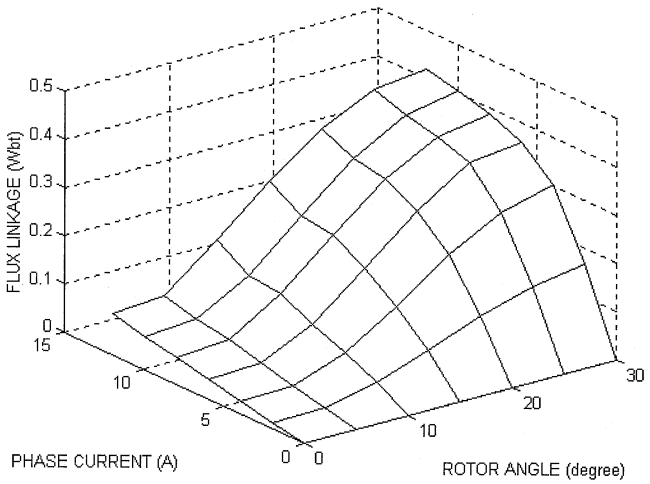

Fig. 3. Input magnetic characteristics.

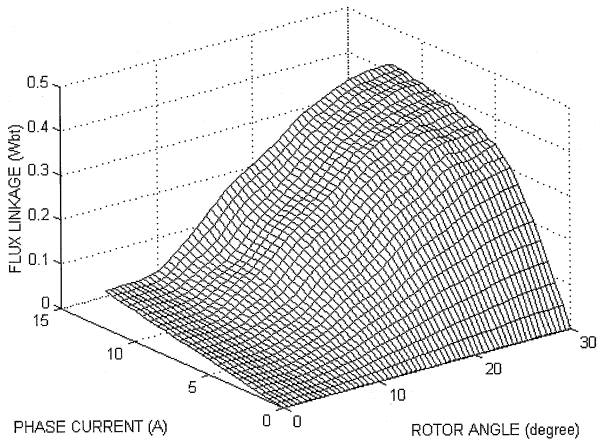

Fig. 4. Interpolated magnetic characteristics.

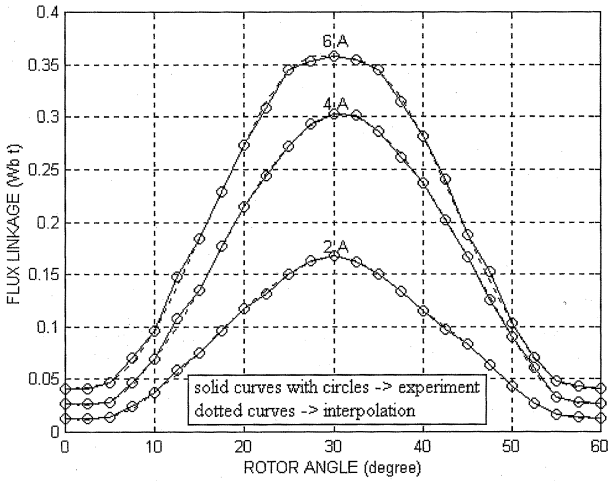

Fig. 5. Comparisons between experimental and interpolated values.

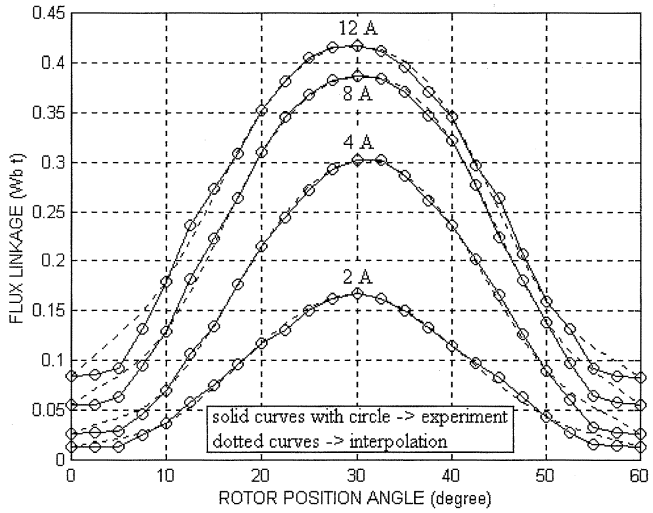

(a)

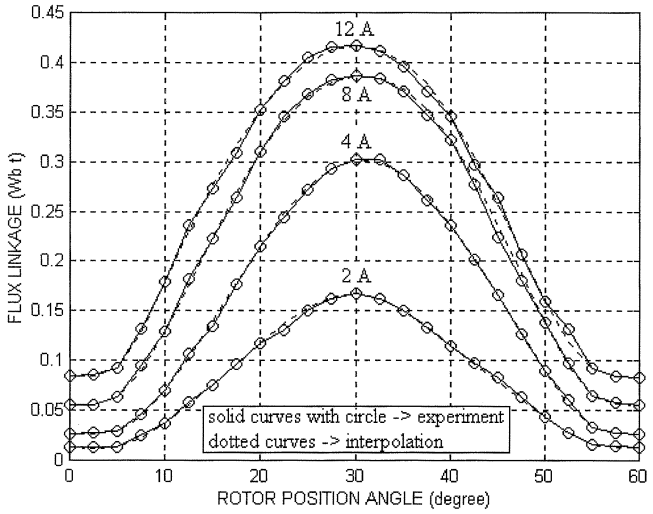

(b)

Fig. 6. Comparisons between experimental and interpolated values (a) The step of 10° for input data without including total flex points (b) Input data to include total flex points.

and r_a is the resistance of winding, u_{cap} is the capacitor voltage, t represents time, u_{dc} is the dc voltage which should be equal to the average value of u_{cap}, u_{mn} represents the maximum line voltage of the ac inputs, m and $n = a, b$, or c but $m \neq n$ and v_R represents the forward voltage drop of the bridge rectifier. Equation (14) can be solved by using the Runge-Kutta method [13].

An accurate model of SRM drives does not only depend on how accurately to describe nonlinear magnetic characteristics in SRM, but also how accurately to establish voltage equation of SRM drives. Equation (14) seems to have two variables that are flux linkage and phase current. Actually, flux linkage is regarded as the solved variable and phase current is only a latent variable that can be computed from flux linkage and rotor position angle, in this study. $d\Psi/d\theta$ may be written the other expression as follows [11].

$$\frac{d\Psi}{d\theta} = \frac{1}{\omega_r}\frac{d\Psi}{dt} = \frac{1}{\omega_r}\left(L\frac{di}{dt} + \omega_r\frac{\partial\Psi}{\partial\theta}\right) = \frac{1}{\omega_r}\left(L\frac{di}{dt} + e\right) \tag{20}$$

where L denotes the phase inductance of SRM and e denotes the back-EMF.

It is seen from (20) that $d\Psi/d\theta$ contains both di/dt and back-EMF. Therefore, (14) can describe the voltage differential equation of SRM drives accurately.

The most general expression for the instantaneous torque produced by one phase at any position is

$$T = \left[\frac{\partial W'}{\partial\theta}\right]_{i_w=const} \tag{21}$$

where W' is the coenergy [11].

The average torque produced by SRM is

$$T_{ave} = \frac{m_p N_r}{2\pi} W \tag{22}$$

where N_r is the number of rotor poles, m_p is the number of phases in SRM drive and W is the total mechanical work done by one phase within one period [11].

As a result, the model proposed in this paper meets the requirement of accurately describing both the nonlinear magnetic characteristics and voltage differential equation of SRM drives.

IV. Application

Using the above model of switched reluctance motor drives with 2-D bicubic spline interpolation, a prototype of switched reluctance motor drives is simulated and reported in this paper. For the prototype of switched reluctance motor drive being studied, its main data are shown as follows.

1) Number of phases $= 4$.
2) Stator poles $= 8$.
3) Rotor poles $= 6$
4) Phase resistance $= 0.687\ \Omega$.
5) Maximum phase inductance/phase current $= 0.0347\ H/12$ A.
6) Minimum phase inductance/phase current $= 0.006\,99\ H/12$ A.
7) Maximum phase inductance/phase current $= 0.0838\ H/2$ A.
8) Minimum phase inductance/phase current $= 0.006\,32\ H/2$ A.
9) Typical on-state voltage of power IGBT $= 1.65$ V.
10) Forward voltage drop of recovery diode $= 0.7$ V.
11) Forward voltage drop of rectifier diode $= 0.7$ V.
12) DC link capacitor $= 1000\ \mu$F.

The magnetic characteristics are shown in Fig. 3.

Fig. 3 illustrates the small amount of input data that describes the nonlinear magnetic characteristics in the switched reluctance motor within the half simulation period. Fig. 4 shows, however, the interpolation results on the basis of Fig. 3.

Fig. 5 shows the comparisons at the step of 2.5° between experimental values and interpolated ones. The interpolated values are based on the experimental values with a step of 5°. It is seen that the interpolated values are virtually identical with the experimental values.

Figs. 3–5 show that the interpolated curves are smooth and accurate and it can describe exactly the nonlinear magnetic characteristics in switched reluctance motors.

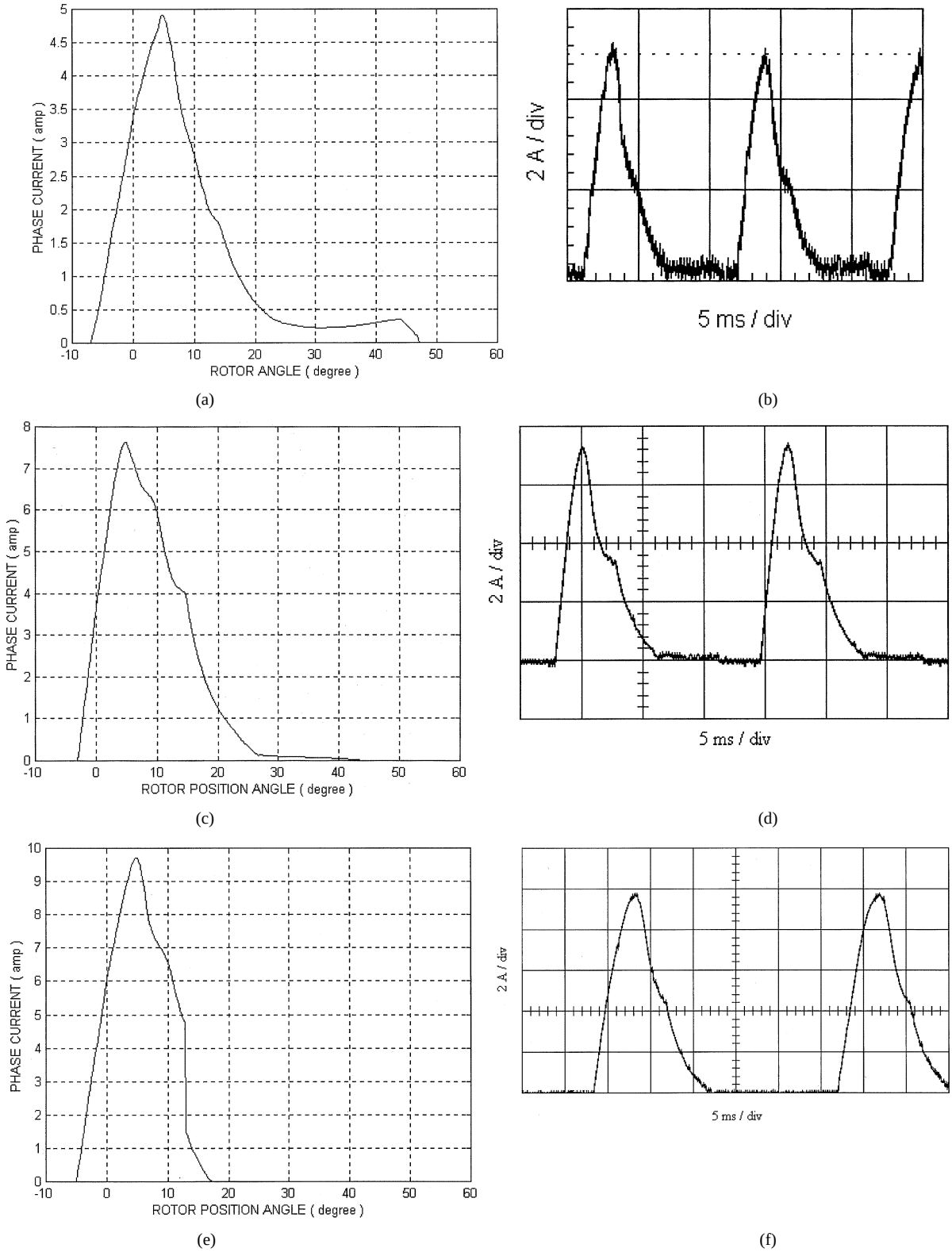

Fig. 7. Simulation and experimental phase current waveforms ("on" = turn on angle, "con" = conduction angle). (a) Simulated phase current waveform at dc-voltage = 22.5 V, on = $-7°$, con = $21°$, speed = 930 rpm. (b) Measured phase current waveforms at dc-voltage = 22.5 V, on = $-7°$, con = $21°$, speed = 930 rpm. (c) Simulated phase current waveform at dc-voltage = 33.4 V, on = $-3°$, con = $18°$ and speed = 600 rpm. (d) Measured phase current waveforms at dc-voltage = 33.4 V, on = $-3°$, con = $18°$ and speed = 600 rpm. (e) Simulated phase current waveform at dc-voltage = 22.5 V, on = $-5°$, con = $18°$ and speed = 350 rpm. (f) Measured phase current waveforms at dc-voltage = 22.5 V, on = $-5°$, con = $18°$ and speed = 350 rpm.

Smaller amount of input data that describes the nonlinear magnetic characteristics is desirable. However, accuracy of interpolation is generally dependent on the amount of input data. Fig. 6(a) shows the comparisons between the experimental and interpolated values at the step of $2.5°$ where the step of input data is $10°$. It is seen that the errors are quite large when rotor

TABLE I
COMPARISONS BETWEEN COMPUTED AND MEASURED TORQUE

Number	1	2	3	4	5	6
Computed average torque T_{ave}	1.158 Nm	0.882 Nm	1.675 Nm	1.326 Nm	2.641 Nm	2.152 Nm
Measured output average T_{out}	0.9 Nm	0.65 Nm	1.45 Nm	1.1 Nm	2.45 Nm	1.95 Nm
T_{ave}-T_{out}	0.258 Nm	0.232 Nm	0.225 Nm	0.226 Nm	0.191 Nm	0.202 Nm

TABLE II
OPERATION CONDITIONS OF TABLE I

Number	Operation conditions
1	input ac phase voltage=15 V, turn-on=-7°, conduction=20°, speed=1000 rpm
2	input ac phase voltage=15 V, turn-on=-4°, conduction=20°, speed=1000 rpm
3	input ac phase voltage=15 V, turn-on=-7°, conduction=20°, speed=800 rpm
4	input ac phase voltage=15 V, turn-on=-4°, conduction=20°, speed=800 rpm
5	input ac phase voltage=15 V, turn-on=-7°, conduction=20°, speed=600 rpm
6	input ac phase voltage=15 V, turn-on=-4°, conduction=20°, speed=600 rpm

position angle changes from 0° to 10° and from 50° to 60°. From the experimental curves in Fig. 6(a), it is observed that magnetic characteristics in SRM drive change much strongly in the above regions. In other words, there are "flex points" in magnetic characteristic curves in the above regions. The input data for the interpolation in Fig. 6(a), however, do not include the above "flex points."

Similarly to Figs. 6(a), 6(b) illustrates the comparisons between the experimental and interpolated values. However, the input data for the interpolation in Fig. 6(b) include the data of "flex points." On the basis of the input data in Fig. 6(a), only the data at the rotor position angle of both 5° and 55° are added in the interpolation of Fig. 6(b). It is seen from Fig. 6(b) that the interpolated curves by using the proposed method can describe nonlinear magnetic characteristics of SRM drive much accurately. As a result, the proposed method needs input data as few as possible, to obtain accurate interpolation results. However, these much few input data must include information of total "flex points."

It is seen that the simulation waveforms are quite similar to the experimental ones, although only a small amount of magnetic data is used. The current step being chosen is 0.25 A and the rotor position angle step is 0.25° for the simulation. However, the current step is 2 A and the rotor position angle step is 5° for the input magnetic data. In other words, the proposed interpolation algorithm and the fine steps ensure a high accuracy, which are essential for a precise simulation for switched reluctance motor drives.

Saturation in SRM drive depends on amplitude of phase current and rotor position. However, saturation in SRM drive is mainly dependent on amplitude of phase current since rotor of SRM rotates. SRM drive will operates at saturation state if phase current is sufficient large. Fig. 7(a) and 7(b) show phase current waveforms at the not high-saturated operation with high speed, whereas Fig. 7(c)–(f) show phase current waveforms at the high-saturated operation with low speed. It is seen that the proposed method can simulate phase currents in SRM drive accurately, regardless of saturated and unsaturated operations.

Table I shows the results of both the computed average electromagnetic torque and the measured output torque. Table II describes the operation conditions of the above simulation and experiment. Table I shows the computation and experimental results of the six operation conditions. The average electromagnetic torque in Table I is computed from (21) and (22) on the basis of the simulated phase current and flux linkage. One knows that viscous friction torque is equal to subtraction of output torque from average electromagnetic torque. Viscous friction torque depends on speed basically, for a specified SRM drive. It is seen from Table I that viscous friction torque is almost the same at the same speed, regardless of the other operation conditions. This shows that the computed electromagnetic torque can describe the real electromagnetic torque produced by SRM drive.

V. CONCLUSION

1) Two-dimensional bicubic spline is chosen as the interpolation function for simulating a switched reluctance motor drive in this study. The key parameter in the study is the flux linkage that is a direct function of both rotor position angle and current. The authors have reported that the use of 2-D biculic spline as the interpolation function can produce excellent matching on the nonlinear magnetic characteristics in switched reluctance motors.
2) The proposed simulation algorithm requires relatively few experimental data and the simulation is accurate and fast.
3) The proposed simulation algorithm enhances the accuracy of simulating switched reluctance motor drives. It can be applicable to computer-aided design, performance prediction and simulation of real-time control.

REFERENCES

[1] D. W. J. Pulle, "New data base for switched reluctance drive simulation," *Proc. Inst. Elect. Eng. B*, vol. 138, pp. 331–337, Nov. 1991.
[2] J. C. Moreira, "Torque ripple minimization in switched reluctance motors via bi-cubic spline interpolation," in *Proc. 23rd Annu. IEEE Power Electron. Spec. Conf. (PESC'92)*, vol. 2, 1992, pp. 851–856.
[3] J. M. Stephenson and J. Corda, "Computation of torque and current in doubly-salient reluctance motors from nonlinear magnetization data," *Proc. Inst. Elect. Eng.*, vol. 126, no. 5, pp. 393–396, 1979.
[4] P. J. Lawrenson, J. M. Stephenson, P. T. Blenkinsop, J. Corda, and N. N. Fulton, "Variable-speed switched reluctance motors," *Proc. Inst. Elect. Eng. B*, vol. 127, pp. 253–265, July 1980.
[5] D. A. Torrey and J. H. Lang, "Modeling a nonlinear variable-reluctance motor drive," *Proc. Inst. Elect. Eng. B*, vol. 137, pp. 314–326, Sept. 1990.
[6] T. J. E. Miller and M. McGilp, "Nonlinear theory of the switched reluctance motor for rapid computer-aided design," *Proc. Inst. Elect. Eng. B*, vol. 137, pp. 337–347, Nov. 1990.
[7] D. A. Torrey, X. M. Niu, and E. J. Unkauf, "Analytical modeling of variable-reluctance machine magnetization characteristics," *Proc. Inst. Elect. Eng.*, vol. 142, pp. 14–22, Jan. 1995.
[8] W. M. Chan and W. F. Weldon, "Development of a simple nonlinear switched reluctance motor model using measured flux linkage data and curve fit," in *Proc. 32nd IAS Annu. Meeting (IAS'97)*, vol. 1, 1997, pp. 318–325.
[9] T. J. E. Miller, M. Glinka, M. McGilp, C. Cossar, G. Gallegos-Lopez, D. Ionel, and M. Olaru, "Ultra-fast model of the switched reluctance motor," in *Proc. IEEE 33rd IAS Annu. Meeting*, vol. 1, 1998, pp. 319–326.

[10] C. Roux and M. M. Morcos, "A simple model for switched reluctance motors," *IEEE Power Eng. Rev.*, pp. 49–52, Oct. 2000.
[11] T. J. E. Miller, *Switched Reluctance Motors and Their Control*. Oxford, U.K.: Magna Physics Publishing and Clarendon Press, 1993.
[12] H. Spaeth, *Two Dimensional Spline Interpolation Algorithms*. Wellesley, MA: K. Peters, 1995.
[13] S. S. M. Wong, *Computational Methods in Physics and Engineering*. Englewood Cliffs, NJ: Prentice-Hall, 1992.

Xiang-Dang Xue received the B.S. degree from Hefei Polytechnic University, China, on August 10, 1984, the M.Sc. degree from Tianjin University, China, on June 22, 1987, and is currently pursuing the Ph.D. in the Department of Electrical Engineering, Hong Kong Polytechnic University.

He has been with the Department of Electrical Engineering, Tianjin University, since July 1987, where he undertook lecturing and researching. His current research is focused on electrical drives, electrical machines, and power electronics.

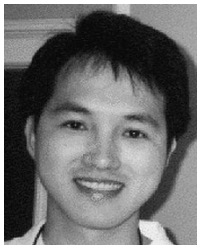

K. W. E. Cheng received the Ph.D. degree from the University of Bath, Bath, U.K., in 1990.

He has been a Project Leader and Principal Engineer with Lucas Aerospace, Ltd., London, U.K. He joined the Hong Kong Polytechnic University in 1997 and is now an Associate Professor. His research interest is all aspects of power electronics and drives. He has published around 100 papers in international journals and conferences.

Dr. Cheng received the IEE Sebastian Z De Ferranti Premium Award in 1995 and the Outstanding Consultancy Award, Hong Kong Polytechnic University, in 2000.

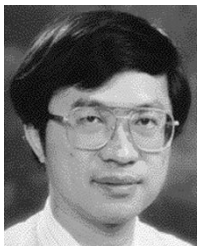

S. L. Ho received the B.Sc. (with first class honors) and Ph.D. degrees from the University of Warwick, Warwick, U.K., in 1976 and 1979, respectively.

He joined Hong Kong Polytechnic in 1979, where he is now a Professor in the Department of Electrical Engineering. His research interests are in the areas of traction engineering, finite element analysis of electromagnetic devices, conditioning monitoring, and phantom loading of electrical machines. He has published around 180 papers in international journals and conferences.